EPR study of a trigonally symmetric Gd^{3+} centre in $RbCaF_3$

1995 J. Phys.: Condens. Matter 7 1417

(http://iopscience.iop.org/0953-8984/7/7/021)

J Phys : Condens. Matter 7 (1995) 1417–1426. Printed in the UK

EPR study of a trigonally symmetric Gd^{3+} centre in $RbCaF_3$

H Takeuchi†, H Ebisu‡ and M Arakawa‡

† Department of Information Electronics, School of Engineering, Nagoya University, Nagoya 464-01, Japan

‡ Department of Physics, Nagoya Institute of Technology, Nagoya 466, Japan

Received 16 November 1994

Abstract. EPR measurements at 300 K have been made on $RbCaF_3$ crystals doped with Gd^{3+} using an X-band spectrometer. Together with the signals from the cubic Gd^{3+} centre, a trigonally symmetric spectrum is observed from as-grown crystals, and is ascribed to a Gd^{3+} ion associated with a nearest Rb^+ vacancy. The separated axial, cubic and hexagonal parameters for the trigonal Gd^{3+} centres in $RbCaF_3$ and $CsCaCl_3$ are discussed in terms of a ligand distortion model in comparison with the parameters for the tetragonal centres in several perovskite fluorides. The larger b_{2a} and b_{4a} for the trigonal centre in $RbCaF_3$ compared with those in $CsCaCl_3$ are explained by the ease of rotational deviations of ligand anions, and are consistent with the higher transition temperature of structural change from cubic to lower symmetry for $RbCaF_3$ than $CsCaCl_3$.

1. Introduction

Gd^{3+} ions substitute selectively for the monovalent or divalent cations in the ABX_3 type crystals with perovskite structure. When a Gd^{3+} ion substitutes for the B^{2+} ion with no charge compensator in its immediate neighbourhood, it forms the cubic centre where surroundings of the Gd^{3+} ion have cubic symmetry. In some matrix crystals, centres with lower symmetries are formed together with the cubic centre. Arakawa *et al* (1982, 1985) reported the tetragonal Gd^{3+} centres in several perovskite fluorides, where Gd^{3+} are associated with the nearest B^{2+} vacancy (Gd^{3+}–V_B centre) or a Li^+ ion at the nearest B^{2+} site (Gd^{3+}–Li^+ centre) due to compensation of the excess positive charges on the Gd^{3+} ions. These tetragonal centres are formed easily in as-grown crystals.

To the authors' knowledge, however, there have been no reports on Gd^{3+} centres associated with nearest A^+ vacancies in perovskite fluorides (Gd^{3+}–V_A centre). Similar Fe^{3+}–V_A and Cr^{3+}–V_A centres have been found in $KZnF_3$ or $KMgF_3$ (Krebs and Jeck 1972, Patel *et al* 1976). As for perovskite chlorides, Vaills and Buzaré (1987) reported the Gd^{3+} centre associated with a nearest Cs^+ vacancy in $CsCaCl_3$ together with the cubic Gd^{3+} centre. The b_2^0 parameter of this centre is very small, that is 3.3×10^{-4} cm^{-1}, as compared with large values of the order of 10^{-2} cm^{-1} to 10^{-1} cm^{-1} for Fe^{3+} and Cr^{3+} centres in perovskite fluorides. It is therefore interesting to observe EPR spectra from some Gd^{3+}–V_A centres in perovskite fluorides from the viewpoint of comparison with the Gd^{3+}–V_{Cs} centre in the perovskite chloride.

The $RbCaF_3$ crystal has a cubic perovskite structure with space symmetry group O_h^1 at room temperature and undergoes a displacive structural phase transition at 193 K. In recent EPR research, we found the existence of a trigonal Gd^{3+} centre in $RbCaF_3$ in its cubic phase. In the present paper, we will report the results of EPR measurements at room temperature for this centre in $RbCaF_3$.

0953-8984/95/071417+10$19.50

In section 3, the spectrum observed will be described by the spin Hamiltonian with trigonal symmetry about the [111] axis. Accurate spin Hamiltonian parameters are presented up to the sixth-rank fine-structure terms. From considerations of charge compensation, the centre is identified to be the Gd^{3+}–V_{Rb} centre. In section 4, the fine-structure terms of the present trigonal centre and the tetragonal centres previously reported are separated into uniaxial, cubic and hexagonal terms. This separation analysis is useful to investigate simultaneously the structures of the complexes with different symmetries, such as cubic, trigonal and tetragonal Gd^{3+} centres. In section 5, the separated parameters for the trigonal centres will be discussed by considering deviations of surrounding ions. First, we consider the relationship between the magnitude of the b_{4c} parameter and Gd^{3+}–F^- distance in the cubic centre. Next, we consider the relationship between the b_{2a} parameter for the trigonal centre and the tolerance factor t that characterizes the ease of rotational distortion of the ligand octahedron. Last, we investigate the relationships among the axial, cubic and hexagonal fine structure parameters for the cubic, trigonal and tetragonal Gd^{3+} centres.

2. Experimental procedures

Single crystals of $RbCaF_3$ doped with 0.3 wt% GdF_3 were grown in graphite crucibles by the flux method using the Bridgman technique. The crystals obtained were transparent and were cleaved easily in the {100} planes.

The measurements were made at room temperatures using a JES-FE1XG EPR spectrometer operating in the X-band at the Centre for Instrumental Analysis in Nagoya Institute of Technology. The sample was mounted on a two-axis goniometer MGM-10 (Microdevice) to be rotated in the microwave cavity with the TE_{011} mode. Numerical computations were performed by the computer at the Computation Centre of Nagoya University. The original software programmed by Takeuchi based on the direct matrix diagonalization method was used for the fitting of the spin Hamiltonian to the spectrum and for graphic output of the calculated angular variation.

3. Results

Typical recorder traces of EPR signals are shown in figure 1. Angular variations of resonant fields for the signals marked with 'T' have extremes in the direction with $\boldsymbol{H}$ parallel to the [111] and [11$\bar{2}$] axes. This shows that the surroundings of the magnetic ions have trigonal symmetry about the [111] axis. The centre is therefore called the 'trigonal centre' hereinafter. In figure 2, signals observed for the centre at 300 K are plotted against external field direction by open circles.

For a trigonal centre, there exist two possible coordinate systems in which fine-structure terms are expressed by Stevens operators O_n^m only with non-negative m. One is the coordinate system A where the principal x, y, z axes are respectively parallel to the [11$\bar{2}$], [$\bar{1}$10], [111] directions. Alternative coordinate system B can be obtained by rotating the system A about the z axis by an angle π, so that the principal x, y, z axes are respectively parallel to the [$\bar{1}\bar{1}$2], [1$\bar{1}$0], [111] directions. We choose the coordinate system A in the present work.

The spectrum observed can be described by the following spin Hamiltonian with $S = \frac{7}{2}$:

$$\mathcal{H} = g_{\parallel}\beta S_z H_z + g_{\perp}\beta(S_x H_x + S_y H_y) + \tfrac{1}{3}b_2^0 O_2^0 + \tfrac{1}{60}(b_4^0 O_4^0 + b_4^3 O_4^3) + \tfrac{1}{1260}(b_6^0 O_6^0 + b_6^3 O_6^3 + b_6^6 O_6^6) \quad (1)$$

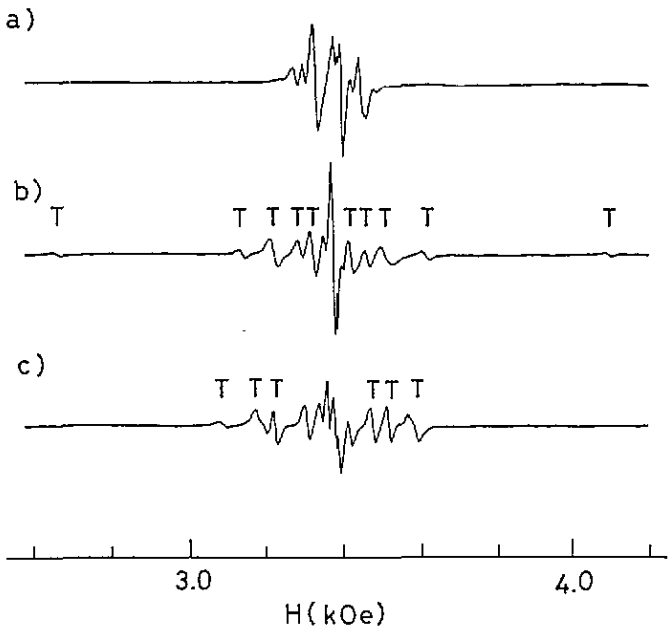

Figure 1. EPR signals observed at 300 K using the X-band spectrometer from an as-grown sample of $RbCaF_3$ doped with Gd^{3+} ions when (a) $H \parallel [001]$, (b) $H \parallel [111]$ and (c) $H \parallel [110]$.

where β is the Bohr magneton and the Stevens operators O_n^m are defined in Abragam and Bleaney (1970). The spin Hamiltonian was fitted to fourteen resonant fields parallel to the [110], [111], [11$\bar{2}$] or [$\bar{1}$10] axes. The root mean square error was 0.1 Gauss. Values obtained for the parameters are listed in table 1. The values in parentheses show least-squares errors for the last numerals. Signs of b_n^m are determined by assuming a positive value for b_4^3 since this parameter is related to the cubic component of the fine-structure term as will be shown by equation (4). The parameters for the cubic Gd^{3+} centres in $RbCaF_3$ and $CsCaCl_3$ and the Gd^{3+}–V_{Cs} centre in $CsCaCl_3$ are also listed in the table for comparison. If we choose the coordinate system B, the signs of the parameters b_2^0, b_4^0, b_6^0 and b_6^6 should be changed with the assumption of positive b_4^3. The coordinate system A may be used for the Gd^{3+}–V_{Cs} centre, although clear discrimination of the coordinate system A or B is not given in the original paper.

In $KMgF_3$ (Abraham *et al* 1971) and $KZnF_3$ (Arakawa *et al* 1979), divalent host cations have too small ionic radii (Sanderson 1967), namely 0.66 Å for Mg^{2+} and 0.74 Å for Zn^{2+}, for substitution by a Gd^{3+} ion (0.97 Å). The Gd^{3+} ions are substituted for the large K^+ ions (1.33 Å). On the other hand, a Ca^{2+} ion (0.99 Å) has a close ionic radius to that of a Gd^{3+} ion, so that the Gd^{3+} ion can be substituted for the Ca^{2+} ion in the $RbCaF_3$ crystal. As a result the Gd^{3+} ion forms the cubic centre, for which the spin Hamiltonian parameters have been reported by Buzaré *et al* (1981). The present trigonal centre in $RbCaF_3$ has the same signs of all the parameters except for b_2^0 as those for the cubic centre. Especially, the sixth-rank fine-structure parameters of the trigonal centre have close values to those of the cubic centre, suggesting that the Gd^{3+} ions are substituted for Ca^{2+} ions in the present trigonal centre.

Trivalent impurity ions substituted for divalent cations in perovskite crystals are often

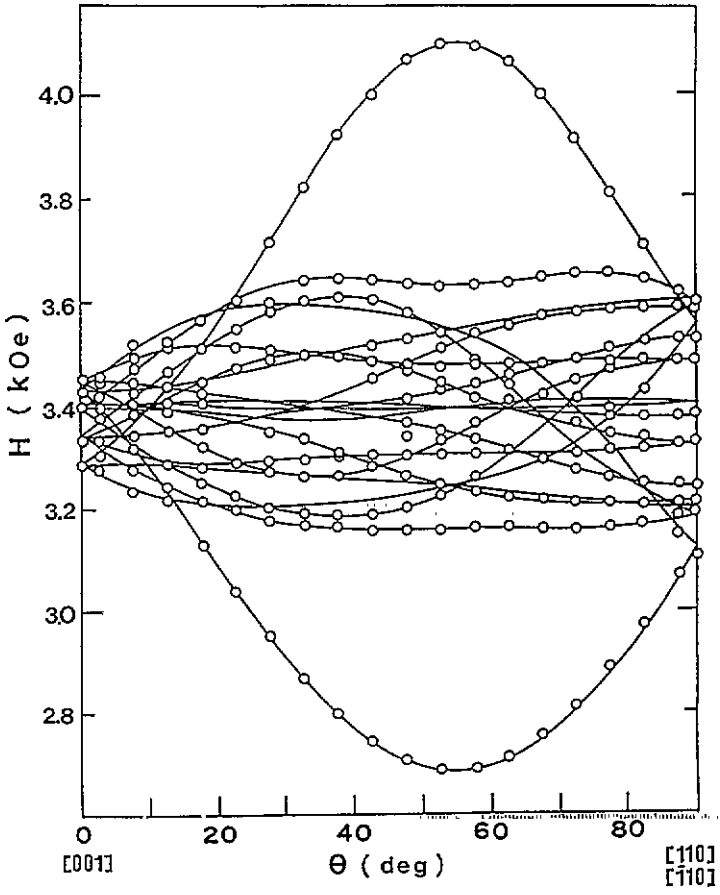

Figure 2. Angular variation of EPR spectrum from the trigonal Gd^{3+} centre at 300 K. Open circles show the signals observed. The full curves denote the calculated resonant fields using the parameters listed in table 1.

Table 1. Experimental values of the spin Hamiltonian parameters for the trigonal Gd^{3+} centre in $RbCaF_3$ and a few related Gd^{3+} centres. b_n^m are in units of 10^{-4} cm^{-1}.

	$RbCaF_3$ Trigonal 300 K	$RbCaF_3$ Cubic 300 K[a]	$CsCaCl_3$ Gd^{3+}–V_{Cs} 300 K[b]	$CsCaCl_3$ Cubic 300 K[b]
$g_\parallel$	1.9918(5)	1.992(1)	—	1.9915(10)
$g_\perp$	1.9917(5)	1.992(1)	—	1.9915(10)
b_2^0	80.1(1)	—	3.3(5)	—
b_4^0	8.36(5)	3.28(3)	9.7(5)	9.2(2)
b_4^3	14(2)	92.8(9)	240(5)	260(6)
b_6^0	1.26(5)	1.48(8)	0.9(5)	0.9(4)
b_6^3	−20(1)	−18(1)	−5.5(5)	−11(4)
b_6^6	13.0(5)	14.2(9)	17(1)	9(3)

[a]Buzaré *et al* (1981).
[b]Vaills and Buzaré (1987).

associated with nearest monovalent cation vacancies for compensation of excess positive charge on the impurity ions (Krebs and Jeck 1972, Patel *et al* 1976, Vaills and Buzaré 1987). The trigonal centre in $RbCaF_3$ may be therefore ascribed to a Gd^{3+} ion associated with a nearest Rb^+ vacancy (hereafter called the Gd^{3+}–V_{Rb} centre).

4. Separation analysis of fine-structure terms

We consider the transformation properties of Stevens operators O_n^m when the xyz coordinate system is rotated about the z axis by angle ϕ into the new $x'y'z'$ coordinate system. In general, the old O_n^m is expressed by a linear combination of $\dot{O}_n^{m'}$ which are Stevens operators in the new coordinate system. We notice the following special cases: the O_n^0 become $\dot{O}_n^0$ for all ϕ; the O_n^m with $m = 3, 4, 6$ become $\dot{O}_n^m$ when $\phi = 2\pi/m$; and the O_n^3 become $-\dot{O}_n^3$ when $\phi = 2\pi/6$.

The spin Hamiltonian which describes the EPR spectrum of a Gd^{3+} ion with cubic symmetry is given by

$$\mathcal{H} = g\beta \boldsymbol{S}\cdot\boldsymbol{H} + \tfrac{1}{60}b_{4c}(O_4^0 + 5O_4^4) + \tfrac{1}{1260}b_{6c}(O_6^0 - 21O_6^4) \tag{2}$$

where the x, y, z axes are parallel to the cubic $\langle 100\rangle$ axes. The terms in b_{4c} and b_{6c} are unchanged in their forms by the $2\pi/4$ rotation of the coordinate system about the z axis. This tetragonality in the cubic centre is equivalent for three possible z axis directions, namely [100], [010] and [001] directions.

Similarly to the trigonal Fe^{3+} centre reported in Takeuchi *et al* (1991), we separate here the fine-structure terms for a trigonal Gd^{3+} centre into uniaxial, cubic and hexagonal terms up to the sixth-rank Stevens operators as follows:

$$\begin{aligned}\frac{1}{3}b_2^0O_2^0 + \frac{1}{60}(b_4^0O_4^0 + b_4^3O_4^3) + \frac{1}{1260}(b_6^0O_6^0 + b_6^3O_6^3 + b_6^6O_6^6)\\ = \frac{1}{3}b_{2a}O_2^0 + \frac{1}{60}\Big[b_{4a}O_4^0 + b_{4c}\Big(-\frac{2}{3}O_4^0 - \frac{40\sqrt{2}}{3}O_4^3\Big)\Big]\\ + \frac{1}{1260}\Big[b_{6a}O_6^0 + b_{6c}\Big(\frac{16}{9}O_6^0 - \frac{140\sqrt{2}}{9}O_6^3 + \frac{154}{9}O_6^6\Big) + b_{6h}O_6^6\Big].\end{aligned} \tag{3}$$

Equation (3) is valid when the following conditions are satisfied:

$$\begin{aligned} b_{2a} &= b_2^0 \qquad b_{4a} = b_4^0 - \frac{1}{20\sqrt{2}}b_4^3 \qquad b_{6a} = b_6^0 + \frac{4}{35\sqrt{2}}b_6^3\\ b_{4c} &= -\frac{3}{40\sqrt{2}}b_4^3 \qquad b_{6c} = -\frac{9}{140\sqrt{2}}b_6^3 \qquad b_{6h} = b_6^6 + \frac{11}{10\sqrt{2}}b_6^3\end{aligned} \tag{4}$$

The terms in b_{2a}, b_{4a} and b_{6a} are unchanged in their forms by any rotations of the coordinate system about the z axis. These terms denote therefore uniaxiality of the wavefunction for magnetic electrons perturbed by the ligand field which includes the effects of the electrostatic crystalline field and covalency. For the wave function with spherical symmetry, that is pure S state, or cubic symmetry, these components of the fine-structure terms vanish. In a low-symmetry centre, b_{4c} represents the mean feature of the tetragonalities about the three cubic axes.

The terms in b_{4c} and b_{6c} are unchanged by the $2\pi/3$ rotation about the z axis. This trigonality is included in the cubic symmetry for the case with vanishing b_{na} and b_{6h}. The parameters b_{4c} and b_{6c} denote the cubic character of the wavefunction. The term in b_{6h} is unchanged by the $2\pi/6$ rotation of the coordinate system about the z axis, so that the term denotes the hexagonality of the Gd^{3+} wavefunction. The terms in b_{na} and b_{6h} arise due to the deformation of the Gd^{3+} wavefunction from cubic symmetry. If we assume for simplicity that the Gd^{3+} wavefunction in a trigonal centre is determined by the coordination of the ligand octahedron, b_{na}/b_{nc} becomes greater for large trigonal elongation or compression of the octahedron and b_{6h}/b_{6c} increases with trigonal compression toward an extreme value for hexagonal symmetry which is completed in a planar sixfold coordination. Values of the axial parameters b_{na} ($n = 2, 4, 6$), cubic parameter b_{nc} and hexagonal parameter b_{6h} calculated by equations (4) are listed in table 2.

Table 2. Values of the uniaxial, cubic and hexagonal parameters for the Gd^{3+} centres with trigonal, tetragonal and cubic symmetries in perovskite type compounds ABX_3 at room temperature. R are the metal–ligand distances in the matrix crystals. b_{na}, b_{nc} and b_{6h} are in units of 10^{-4} cm^{-1}.

Centre	R (Å)	T (K)	b_{2a}	b_{4a}	b_{6a}	b_{4c}	b_{6c}	b_{6h}	Symmetry
Cubic Gd^{3+}									
$RbCdF_3$	2.200[a]	295[b]	—	—	—	−4.44	0.82	—	Cubic
$RbCaF_3$	2.227[a]	300[c]	—	—	—	−4.92	0.83	—	Cubic
$CsCdF_3$	2.230[a]	296[b]	—	—	—	−4.82	0.86	—	Cubic
$CsCaF_3$	2.262[a]	296[b]	—	—	—	−5.49	0.89	—	Cubic
$CsCaCl_3$	2 691[d]	300[e]	—	—	—	−13.8	0.5	—	Cubic
Gd^{3+}–V_A									
$RbCaF_3$		300	80.1	7.87	−0.36	−0.74	0.91	−2.5	Trigonal
$CsCaCl_3$		300[e]	3.3	1.2	0.46	−13	0.25	13	Trigonal
Gd^{3+}–V_B									
$RbCdF_3$		302[f]	−291.3	6.20	−0.09	−8.32	0.90	—	Tetragonal
$RbCaF_3$		297[f]	−274.9	5.72	0.00	−8.58	0.83	—	Tetragonal
$CsCdF_3$		300[f]	−315.1	6.90	−0.09	−9.28	0.90	—	Tetragonal
$CsCaF_3$		298[f]	−314.7	6.91	−0.08	−9.96	0.90	—	Tetragonal
Gd^{3+}–Li^+									
$RbCdF_3$		302[f]	−330.2	5.26	0.04	−7.66	0.82	—	Tetragonal
$RbCaF_3$		297[f]	−318.2	5.84	−0.05	−8.80	0.91	—	Tetragonal
$CsCdF_3$		300[f]	−379.8	7.14	−0.08	−9.40	0.90	—	Tetragonal
$CsCaF_3$		298[f]	−388.3	8.17	−0.03	−10.88	0.88	—	Tetragonal

[a]Rousseau *et al* (1978).
[b]Arakawa *et al* (1982).
[c]Buzaré *et al* (1981).
[d]Vaills *et al* (1986).
[e]Vaills and Buzaré (1987).
[f]Arakawa *et al* (1985).

Arakawa *et al* (1985) reported fine-structure parameters for the tetragonal Gd^{3+} centres associated with nearest divalent cation vacancies (Gd^{3+}–V_B centre) or Li^+ ions at the nearest divalent cation site (Gd^{3+}–Li^+ centre) in several perovskite fluorides ABF_3. In the later work (Takeuchi *et al* 1987), the fine-structure terms with tetragonal symmetry for the Gd^{3+} centres in $RbCdF_3$ and $CsCdF_3$ were separated into uniaxial and cubic terms to compare them with those of the cubic and orthorhombic Gd^{3+} centres. Here, in the same way we calculate the uniaxial and cubic parameters at room temperature for the tetragonal centres in $RbCaF_3$ and $CsCaF_3$. Results are summarized in table 2.

Except for b_{2a}, the axial and cubic parameters for the trigonal centre in $RbCaF_3$ have the same signs as those for the tetragonal centre in the same matrix. The values of b_{2a} for the trigonal centres in both $RbCaF_3$ and $CsCaCl_3$ are positive as contrasted with negative values for the tetragonal centres. The trigonal centre in $CsCaCl_3$ has very small b_{2a} value and a close value of b_{4c} to that of the cubic centre. On the other hand, b_{2a} for the trigonal centre in $RbCaF_3$ is considerably larger than that for $CsCaCl_3$. This suggests that the surroundings of the Gd^{3+} ion in $RbCaF_3$ are much more distorted from cubic configuration than those in $CsCaCl_3$.

5. Discussion

A Gd^{3+} ion has ionic radius close to those of a Ca^{2+} and a Cd^{2+} ion. In the uncompensated Gd^{3+} centres (cubic centre) ligand anions are expected to deviate from the face centre points toward the Gd^{3+} ion due to excess positive charge on the Gd^{3+} ion. Rewaj *et al* (1992) reported that each magnitude of b_4^4 ($= 5b_{4c}$) for the uncompensated Gd^{3+} centres in $CsCaF_3$, $RbCaF_3$ and $RbCdF_3$ increases with increasing hydrostatic pressure. This result suggests that $|b_{4c}|$ increases with decreasing Gd^{3+}–F^- distance in perovskite fluorides. As the b_{4c} at 4.2 K are -6.90 ± 0.02 for $CsCaF_3$ and -6.10 ± 0.04 for $CsCdF_3$ in units of 10^{-4} cm^{-1} (Allsopp *et al* 1987), the Gd^{3+}–F^- distance for $CsCaF_3$ is considered to be smaller than that for $CsCdF_3$. Allsopp *et al* estimated the Gd^{3+}–F^- distances R to be 2.204 Å for both $CsCaF_3$ and $CsCdF_3$ at 4.2 K using the Baker model in the analysis of the nearest superhyperfine interaction (SHFI) parameters A_s and A_p determined from their ^{19}F ENDOR measurements. Metal–ligand distances R_0 in matrices are 2.257 Å for $CsCaF_3$ and 2.226 Å for $CsCdF_3$ at 4.2 K, so that larger fluorine deviation toward the Gd^{3+} ion takes place for the matrix crystal with larger lattice constant. Experimental values of A_s are $-3.869 \pm$ 0.004 MHz for $CsCaF_3$ and -3.759 ± 0.003 MHz for $CsCdF_3$. Considering only A_s, which may be more reliable for estimation of metal–ligand distances than A_p, we obtain a Gd^{3+}–F^- distance for $CsCaF_3$ smaller than that for $CsCdF_3$. The larger $|b_{4c}|$ for $CsCaF_3$ than that for $CsCdF_3$ is consistent with the larger $|A_s|$ for $CsCaF_3$. Thus, the stressed EPR results and the conclusive ligand-ENDOR results lead us to the fact that $|b_{4c}|$ increases with decreasing Gd^{3+}–F^- distance in perovskite fluorides. The $|b_{4c}|$ values for the cubic Gd^{3+} centre in $CsCaCl_3$ are about a factor of 2.5–3 larger than those in the fluorides. This suggests that the $4f^7$ electrons are affected by cubic deformation of outer 5s, 5p shell partly due to covalency.

From ^{19}F-ENDOR measurements for the Fe^{3+}–V_K centre in $KZnF_3$, Krebs and Jeck (1972) found tilts of the Fe^{3+}–F^- bond directions apart from the cubic axes. Similar tilts of the Cr^{3+}–F^- bond directions were found in the ^{19}F-ENDOR measurements for the Cr^{3+}–V_K centre in K_2ZnF_4 (Takeuchi *et al* 1982, Takeuchi 1983). Recently, Takeuchi *et al* (1991) reported EPR results for the Fe^{3+}–V_{Rb} centre in Rb_2ZnF_4, and analysed the spin Hamiltonian parameters on the basis of the ligand distortion model where the front fluorines are deviated toward the opposite directions to the A^+ vacancy. Similar deviations of ligand ions are therefore expected to happen in the Gd^{3+}–V_A centres in $RbCaF_3$ and $CsCaCl_3$.

The space between A^+ and X^- ions relative to the metal–ligand distance R ($= a/2$) of a matrix crystal is given by $\sqrt{2} - (r_A + r_X)/R$, where r_A and r_X are respectively the ionic radii of the A^+ and X^- ions. Estimated values are 0.16 for $RbCaF_3$ and 0.12 for $CsCaCl_3$ with the values $r_{Rb} = 1.47$Å and $r_{Cs} = 1.67$Å. These values suggest that in the Gd^{3+}–V_A centres the tilt of the bond direction for the front ligand by the presence of the A^+ vacancy takes place more easily in $RbCaF_3$ than in $CsCaCl_3$. The larger b_{2a} value for $RbCaF_3$ than that for $CsCaCl_3$ is consistent with the larger relative space for ligand deviation along the A^+–X^- direction.

By decreasing temperature or increasing pressure the B^{2+}–X^- distance is decreased and in some cases the X^- ion may be distorted from the face centre of the cubic unit cell. Structural instability of the perovskite crystal ABX_3 is related to the tolerance factor defined by

$$t = \frac{r_A + r_X}{\sqrt{2}(r_B + r_X)} \qquad (5)$$

where r_A, r_B and r_X are respectively the ionic radii of the A^+, B^{2+} and X^- ions. This can be seen from figure 3, where the transition temperatures from cubic to lower phase are plotted for ABF_3 (A = K, Rb; B = Ca, Cd) and for $ACaCl_3$ (A = K, Rb, Cs). Each transition temperature for the fluoride or chloride increases almost linearly with decreasing t. The X^- ion can deviate in the A_4X face plane more easily for the crystal with smaller t. The ligand octahedron in the Gd^{3+}–V_{Rb} centre in $RbCaF_3$ may be more distorted than that in the Gd^{3+}–V_{Cs} centre in $CsCaCl_3$, as the former has a smaller tolerance factor and a larger relative space for deviation along the A^+–X^- direction than the latter. Thus, the magnitude of b_2^0 of the trigonal Gd^{3+} centre is related to the tolerance factor that characterizes the ease of the rotational distortion of anion octahedron.

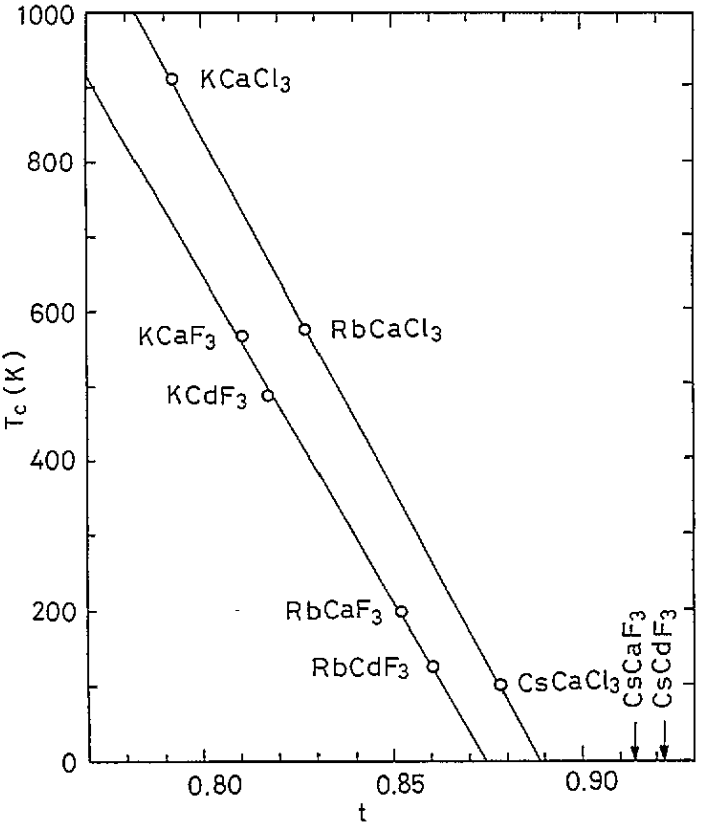

Figure 3. The variation of the transition temperatures for structural changes from cubic to low symmetry against the tolerance factor t. The full curves are guides for the eyes.

For the tetragonal centres, b_{4a} increases roughly with increasing $|b_{2a}|$. The ratios b_{4a}/b_{2a} for the Gd^{3+}–V_B centres are almost constant (−0.021 to −0.022), and those for the Gd^{3+}–Li^+ centres are in the range −0.016 to −0.021. A similar trend was not found for b_{6a} as these values are too small. In contrast to the tetragonal centres, the ratio b_{4a}/b_{2a} for the trigonal centre in $RbCaF_3$ is positive and its magnitude is about a factor of five larger than those of the tetragonal centres. b_{6a} has a considerably larger magnitude as compared with the tetragonal centres. Thus, in the trigonal centre the fourth and sixth axial components of the fine-structure terms are significant in description of the spectrum.

There exists a characteristic trend that $|b_{4c}|$ for the trigonal centres are smaller and those for the tetragonal centres are larger than $|b_{4c}|$ for the cubic centres in the same matrices. It is considered by the ligand distortion model that in the trigonal centre the distances to six ligands become larger by the large deviations of the front ligands away from the vacancy and a small deviation of Gd^{3+} toward the vacancy. In contrast to b_{4c}, the parameter b_{6c} is approximately constant among the cubic, tetragonal and trigonal centres in the fluoride matrices. This parameter may not be affected so much by the distortion of surroundings. This constancy can be used as a measure of a well fitted set of experimental values.

6. Conclusions

The trigonal centre in $RbCaF_3$ has been identified as the substitutional Gd^{3+} centre at a Ca^{2+} site associated with a nearest Rb^+ vacancy. The large b_{2a} value compared with that for the Gd^{3+}–V_{Cs} centre in $CsCaCl_3$ is explained by large ligand deviations from cubic configuration due to the lack of positive charge at the Rb^+ vacancy. The Gd^{3+}–V_A centre with larger b_{2a} has larger space between the A^+ and X^- ions. This trend is related to the higher transition temperature from cubic to lower symmetry of the matrix crystal for the trigonal centre with larger b_{2a}. For the trigonal Gd^{3+} centre the terms in b_{4a} and b_{6a} are significant compared with those for the tetragonal centres. The magnitudes of b_{2a}, b_{4a} and b_{4c} for the tetragonal centres increase roughly with increasing lattice constant of the matrix crystals. The constancy of b_{6c} among the cubic, trigonal and tetragonal Gd^{3+} centres in perovskite fluoride matrices can be used as a measure of a well fitted set of experimental values.

Acknowledgments

The authors thank Dr Masahiro Mori for useful discussions. This work has been supported by a Grant-in-Aid for Scientific Research on Priority Areas 'New Development of Rare Earth Complexes' No 06241232 from the Ministry of Education, Science and Culture.

References

Abragam A and Bleaney B 1970 *Electron Paramagnetic Resonance of Transition Ions* (Oxford: Clarendon)
Abraham M M, Finch C B, Kolopus J L and Lewis J T 1971 *Phys. Rev.* B **3** 2855–64
Allsopp R A, Baker J M, Bluck L J and Buzaré J Y 1987 *J. Phys. C: Solid State Phys.* **20** 451–62
Arakawa M, Aoki H, Takeuchi H, Yosida T and Horai K 1982 *J. Phys. Soc. Japan* B **51** 2459–63
Arakawa M, Ebisu H and Takeuchi H 1985 *J. Phys. Soc. Japan* B **54** 3577–83
Arakawa M, Ebisu H, Yosida T and Horai K 1979 *J. Phys. Soc. Japan* B **46** 1483–7
Buzaré J Y, Fayet-Bonnel M and Fayet J C 1981 *J. Phys. C: Solid State Phys.* **14** 67–81
Krebs J J and Jeck R K 1972 *Phys. Rev.* B **5** 3499–505

Patel J L, Davies J J, Cavenett C, Takeuchi H and Horai K 1976 *J. Phys. C: Solid State Phys.* **9** 129–38
Rewaj T, Krupski M, Kuriata J and Buzaré J Y 1992 *J. Phys.: Condens. Matter* **4** 9909–18
Rousseau J J, Leblé A and Fayet J C 1978 *J. Physique* **39** 1215–23
Sanderson R T 1967 *Inorganic Chemistry* (New York: Reinhold)
Takeuchi H 1983 *Res. Bull., College Gen. Educ. Nagoya Univ.* B **27** 41–9
Takeuchi H, Arakawa M, Aoki H, Yosida T and Horai K 1982 *J. Phys. Soc. Japan* **51** 3166–72
Takeuchi H, Arakawa M and Ebisu H 1987 *J. Phys. Soc. Japan* **56** 4571–80 (erratum 1990 **59** 2297)
—— 1991 *J. Phys.: Condens. Matter* **3** 4405–20
Vaills Y and Buzaré J Y 1987 *J. Phys. Chem. Solids* **48** 363–70
Vaills Y, Buzaré J Y, Gibaud A and Launay Ch 1986 *Solid State Commun.* **60** 139–41